How High Local Charge Carrier Mobility and an Energy Cascade in a Three-Phase Bulk Heterojunction Enable >90% Quantum Efficiency

*Timothy M. Burke, and Michael D. McGehee**

The best organic photovoltaics (OPV) with bulk-heterojunction (BHJ) morphologies based on partially phase separated donor:acceptor blends now have over 9% power conversion efficiency and field-independent internal quantum efficiencies over 90%.[1] However, an incomplete understanding of how free charges are photogenerated in BHJ devices hinders the rational design of better materials still needed for OPV to reach commercial viability. Recent attention has turned to the ubiquitous molecular mixing between fullerenes and polymers, which results in a molecularly-mixed region in BHJ systems along with the typically pictured aggregated donor and acceptor phases.[2–4] A schematic of this three-phase morphology is shown in **Figure 1**. Understanding the role of the amorphous mixed region in charge generation is important since it makes up a large fraction of the film volume in many polymer-fullerene BHJ systems. In P3HT:PCBM solar cells, for example, a study found that only about 50% of the P3HT was aggregated while the high performing system PTB7:$PC_{71}BM$ was found to consist entirely of an amorphous mixed region with embedded $PC_{71}BM$ clusters.[5,6] Work by many groups has shown that the presence and composition of the mixed region can have a dramatic impact on device performance.[7–9] This impact could be due to the fact that the mixed region has been reported to have energy levels that are shifted with respect to the aggregated phases, producing an energy cascade that assists in free charge generation.[8,10–12] For example, PCBM has been shown to have a 100–200 meV shift in electron affinity upon aggregation and P3HT, the prototypical OPV donor, displays a 300 meV change in optical bandgap between amorphous and crystalline regions.[6,10,13]

In this report, we studied the role of the mixed region in assisting geminate splitting using Kinetic Monte Carlo (KMC) simulations of idealized trilayer (pure donor/mixed region/pure acceptor) morphologies. We find that efficient geminate separation efficiency is predicted by KMC when fast, local (monomer-scale) charge carrier mobilities are taken into account. Additionally, we demonstrate that a 200 meV energetic offset between the mixed and pure regions in the simulated trilayer devices greatly decreases the local mobilities and Charge Transfer state lifetimes required for efficient charge generation.

T. M. Burke, Prof. M. D. McGehee
Stanford University
476 Lomita Mall, Stanford, CA, 94305, USA
E-mail: mmcgehee@stanford.edu

DOI: 10.1002/adma.201304241

Excitons in BHJ systems are known to dissociate at the heterojunction between the donor and acceptor materials into a hole (positive polaron) residing on the donor and an electron (negative polaron) residing on the acceptor.[14,15] However, due to the low dielectric constant of organic semiconductors, these charges are not free and instead form a coulombically bound radical pair with a binding energy that is calculated to be around 350 meV (assuming $\varepsilon_r = 4$ and a typical intermolecular spacing of 1 nm).[14] This geminate pair needs to become separated by approximately 12 nm before its binding energy is equal to the thermal energy at room temperature, the point at which the charges are typically considered to be free, although entropic considerations as well as the presence of disorder could reduce this distance to about 5 nm.[14] In either case, the formation of free charges is a kinetic competition between the rate at which geminate pairs split via a combination of drift and diffusion, which is determined by the electron (μ_e) and hole (μ_h) mobilities, and the rate at which they recombine when they are on neighboring molecules, which has a characteristic lifetime τ_{ct}. When the electron and hole are adjacent to each other and could immediately recombine, the pair is said to form a Charge Transfer (CT) state.[16] Given values for μ and τ_{ct}, one can predict the fraction of photons that result in free charges either by using the analytical Onsager-Braun theory or by simulating and averaging many individual electron and hole trajectories using the Kinetic Monte Carlo technique.[17–19] A troubling issue is that when one uses experimental values for the bulk mobility in BHJs on the order of 10^{-4} cm^2/Vs or lower and an estimate for τ_{ct} obtained from photoluminescence decay or transient absorption measurements (1–10 ns), the predicted device quantum efficiency is typically less than 10% at short circuit conditions and increases significantly when one simulates a device under reverse bias by adding a strong electric field.[14,20] This inefficient, field-dependent splitting is characteristic of a process where the mobility and lifetime of the geminate pairs are not large enough for the charges to separate on their own. When splitting does occur, it is primarily due to the built-in field of the BHJ overcoming the pair's binding energy and pulling the electron and hole apart. The strength of this field decreases at forward bias, making charge generation less efficient as the cell approaches open circuit and reducing the fill factor. Thus, while this model can explain the poor performance of low-efficiency OPV material systems like MDMO-PPV:PCBM, which do show field-dependent geminate splitting, it stands in sharp contrast to the field-independent internal quantum efficiencies near or above 90% observed experimentally in champion polymer systems like PCDTBT, PTB7 and PBDTTPD.[7,14,21–24]

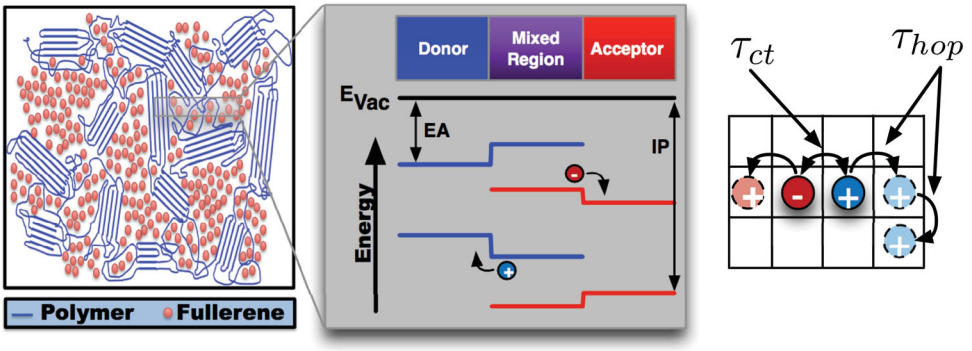

Figure 1. (left) Schematic of a BHJ solar cell including the mixed region. Potential shifts in the local energetic landscape at the border between the donor, mixed and acceptor phases are shown in detail. EA is the electron affinity, IP is the ionization potential. (right) A 2D schematic of the Kinetic Monte Carlo simulation method showing the rates for hopping and recombination.

The inability to reconcile experimental quantum efficiency measurements of high-performing systems with Monte Carlo simulations has led many groups to propose additional theories about what factors the simulations are lacking that could explain the discrepancy. One current theory is that efficient geminate splitting requires the presence of excess thermal energy, although this is under debate and sub-bandgap quantum efficiency measurements suggest that excess energy is not necessary in some systems.[25–28] Previous Kinetic Monte Carlo studies have also investigated the potential effects of charge carrier delocalization, energetic disorder, molecular dipoles and dielectric reorganization and found that, while each can improve geminate splitting, none were able to account for a 90%, field-independent IQE without assuming a value for τ_{ct} that is orders of magnitude longer than experimentally reported.[8,14,20,29,30]

Our simulation environment is similar to that previously reported and is described in the experimental section and Supporting Information, but a brief summary is useful to aid in interpreting the results.[19] The KMC algorithm simulates geminate splitting by iteratively tracking the progress of many individual electron and hole trajectories as the carriers hop along a three dimensional lattice of sites that represent donor or acceptor molecules (see Figure 1). When multiple kinetic processes could occur in competition, KMC chooses one at random in such a way that faster processes occur correspondingly more often. The rate of hopping events was determined by the Miller Abrahams (M-A) hopping expression, since it is computationally simple and has been used extensively to model geminate splitting.[19,20,29,31–33] The M-A model assumes that energetically downhill hops proceed at a constant rate while uphill hops are thermally activated:

$$k_{hop} = \begin{cases} k_0 & \Delta E \leq 0 \\ k_0 exp(\frac{-\Delta E}{kT}) & \Delta E > 0 \end{cases}$$

The energy term includes contributions both from the electric field and the Coulomb potential and can be written, following Peumans as:

$$E = -\frac{q^2}{4\pi\varepsilon_0\,\varepsilon_r\,r_{eh}} - q\,\vec{F}\cdot\vec{r}_{eh} + U_{LUMO}(\vec{r}_e) - U_{HOMO}(\vec{r}_h),$$

where q is the elementary charge, ε the dielectric constant, F the electric field and r_{eh} the geminate pair separation vector.[19] U specifies the energy levels of the electron and hole lattice sites.

It is important to note that, at this nanometer length scale, hole transport from the mixed to aggregated regions could occur along a single polymer chain, potentially resulting in extremely high local hole mobilities.[34] To study this, we fixed the electron mobility at 4×10^{-5} cm^2/Vs in our simulations and varied the hole mobility to investigate the combination of a 3 phase morphology and fast local hole motion. To make the simulation amenable to analytical analysis, we modeled each region as a homogenous average material without energetic disorder. In the Supplemental Information we show simulations that include energetic disorder and a mixed region composed of a blend of donor and acceptor molecules that only transport one type of charge carrier (Supporting Information, Figure S1 and S3-S5). These additions to the model affect the results in a much smaller manner than the effects we emphasize in the main text. We did find, though, that all the simulations depended sensitively on the choice of average carrier mobility and recombination lifetime, as illustrated in **Figure 2**a. For a fixed mixed region width of 3.2 nm and CT state lifetime of 5 ns, the apparent effect of the energy cascade, measured as the difference in splitting efficiency between its presence and absence, varies from imperceptible when $\mu_h = 4 \times 10^{-4}$ cm^2/Vs to fully accounting for >90% field-independent geminate splitting when μ_h = 4 cm^2/Vs. Thus, before presenting the results, a discussion is in order of what is known experimentally about μ and τ_{ct}.

Previous KMC studies have tended to use mobility values designed to reproduce bulk diode mobilities measured in BHJ devices, with values on the order of 10^{-3}–10^{-4} cm^2/Vs. **Table 1** reports the mobilities and lifetimes required in those studies to predict 90% IQE at short circuit conditions. Carrier mobility in KMC simulations is specified by giving an absolute rate for hops between lattice sites (units of hops per second). A standard result for three-dimensional random walk simulations relates this rate to the diffusion coefficient, which is linked to the experimentally measurable mobility using the Einstein relation (see the Supporting Information for complete details). It is important to note, however, that charge transport in disordered organic semiconductors is not characterized by a single mobility across all length scales.[34,35] Long-range, bulk mobility

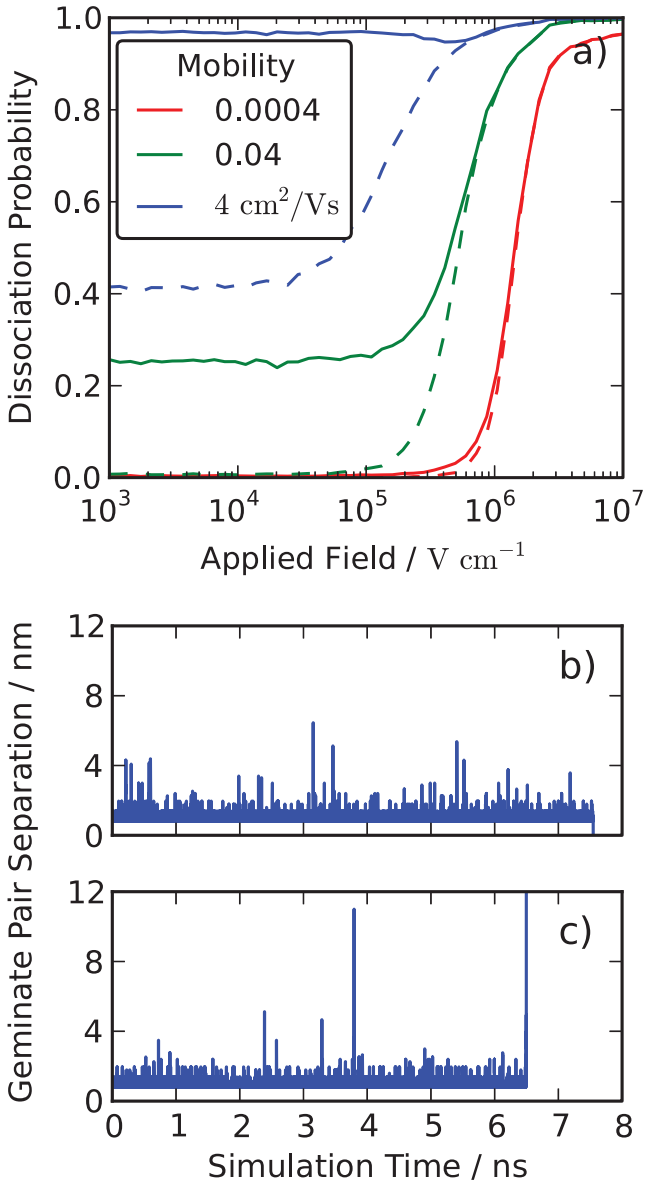

Figure 2. a) The field dependent dissociation of geminate pairs in a mixed region 3.2 nm wide with the electron mobility fixed at 4×10^{-5} cm^2/Vs and the hole mobility varied from 4×10^{-4} cm^2/Vs up to 4 cm^2/Vs, τ_{ct} is fixed at 5 ns. The dashed lines are without an energetic offset, the solid lines with a 200 meV energetic offset. b&c) The separation distance evolution between the electron and hole in a typical geminate splitting simulation with τ_{ct} = 10 ns and $\mu_e = \mu_h$ = 1 cm^2/Vs. Figure 2b ended in recombination, 2c in splitting.

is limited by sparse, deep traps whereas short-range mobility is determined by the charges' intrinsic hopping rates.[34,35] Consequently, the mobility value measured in a space-charge-limited current measurement or time of flight measurement is lower than that measured by time resolved microwave conductivity, which is lower still than that measured by time resolved terahertz conductivity (TRTC).[7,36,37] As one probes shorter length scales, the carrier mobility increases since the probability of it encountering a trap during the measurement is lower. Studies have shown that only the high frequency terahertz conductivity

Table 1. Lifetime and mobility values that were required in previous KMC studies to predict 90% geminate splitting at short circuit conditions (field of 10^5 V/cm). Conditions required to obtain field independence are noted in footnotes.

Group	Mobility [cm^2/Vs]	Lifetime [ns]	90% IQE Predicted	Field Independent
Janssen 2005[20]	3×10^{-5}	1000	Yes	No
Groves 2008[40]	2×10^{-3}	2000	Yes	No
Deibel 2009[29]a,	3×10^{-5}	10000	Yes	Yes
Wojcik 2010[31]	5×10^{-3}	100	Yes	No
Groves 2013[8]b,	6×10^{-4}	100	Yes	Yes

a)Modeled charges delocalized along 10 monomer units. b)Modeled a mixed region 1 nm wide with energetic offset of 300 meV.

gives information directly on the intrinsic hopping rate, while the other techniques report values limited by slow but infrequent processes (compared to the hopping rate).[36]

A complete device simulation that includes all of the mechanisms by which high local mobilities naturally decay into low bulk mobilities over longer length scales should fully reproduce this hierarchical behavior, but for focused simulations solely of geminate splitting the question arises as to whether bulk mobility values or single-hop terahertz mobility values are more appropriate. The answer depends on what role the mobility parameter is playing in the simulation. To elucidate this role, the separation as a function of time between two typical geminate pairs (τ_{ct} = 10 ns, $\mu_e = \mu_h$ = 1 cm^2/Vs) is plotted in Figure 2b and 2c. As can be seen, the charges, due to their strong binding energy, spend the majority of their time right next to each other, with brief, relatively infrequent separations. Each of these separations, which we call splitting attempts, can end either with the charges becoming free or with them again becoming nearest neighbors, reforming the CT state. Recombination is assumed to be a nearest-neighbor process, so once the charges take one hop apart they cannot recombine until they first meet each other again. The probability that the charge carriers, once they are no longer nearest neighbors, separate completely without meeting again turns out to be largely independent of both the carrier mobility and the recombination lifetime (see Supporting Information, Figure S1, S4, and S5). It is independent of τ_{ct} since recombination only happens between nearest neighbors. It is independent of μ since the mobility is modeled as being isotropic so the carrier mobility just sets the timescale for each hop, it does not make the carriers more likely to hop in one direction (toward each other, reducing their separation) than in another direction (away from each other, increasing their separation).

We call the probability that an electron and hole successfully escape from their mutual attraction in a single splitting attempt P_{esc}. Since P_{esc} does not depend on either the carrier mobility or lifetime, it must be a constant determined by the device's energetic landscape (see Supporting Information, Figure S2 and S4). The geminate splitting efficiency is determined by the number of splitting attempts each geminate pair makes, on average, before recombining and the probability that any single attempt is successful. The number of attempts is set by the product of μ and τ_{ct} since when the carriers are nearest

Table 2. Literature measurements for local mobility (measured using time resolved terahertz spectroscopy) and the geminate pair lifetime (measured using transient absorption or transient photoluminescence).

Morphology	Local Mobility [cm^2/Vs]	Geminate Pair Lifetime [ns]
P3HT/PCBM[38,41–43]	0.1 – 30	3
AFPO-3/PCBM[43]	0.73–1	n/a
ZnPc/C60[44]	0.4	n/a
TQ1/PCBM[45]	0.1	n/a
PF10TBT/PCBM[39]	n/a	4

neighbors, they can either recombine or attempt to split again. The probability of them recombining is set by the kinetic competition between the rate of a single hop apart, set by μ, and the rate of recombination, set by $1/\tau_{ct}$ (full derivation in Supporting Information).

We conclude that the carrier mobility in a KMC simulation of geminate splitting primarily sets the branching ratio between recombination and another splitting attempt when the electron and hole are nearest neighbors. Once the carriers are no longer next to each other, whether they continue to split until they are free depends mainly on the energetic landscape. The fact that geminate splitting does not depend on the average value of the mobility for more than a single hop means that the appropriate mobility value is not the bulk mobility but the value for a single carrier hop, which is given by TRTC measurements. Put another way, using the bulk mobility will dramatically underestimate the number of splitting attempts each geminate pair makes but will reproduce the bulk mobility over long length scales. Using the terahertz mobility will correctly predict the geminate splitting efficiency but will overestimate the bulk mobility if combined with a simplified morphology.

Choosing the correct mobility value is critically important because the TRTC mobilities of BHJ material systems (shown in **Table 2**) are between 0.1 and 30 cm^2/Vs, which is 2–5 orders of magnitude larger than the bulk mobility values. This explains why previous authors were forced to assume long, physically unlikely, recombination lifetimes to reproduce experimental geminate splitting efficiencies (see Table 1). Because the geminate splitting efficiency depends on the product $\mu\tau_{ct}$, an underestimate of μ results in an overestimate of τ_{ct} by the same amount in order that the product of the two be sufficiently large to ensure many splitting attempts per geminate pair.

Having established the appropriate range of values for μ from experiments reported in literature, we now do the same for τ_{ct}, which specifies the rate of recombination for electrons and holes that reside on neighboring molecules. This rate is not the same as the free carrier lifetime measured with a technique like transient photovoltage (TPV). TPV lifetimes are dominated by the rate at which already-free carriers encounter each other rather than the rate at which they recombine once they have become nearest neighbors. It is this latter rate that is needed for KMC simulations. There are far fewer reports of CT state (nearest neighbor) lifetimes, which are primarily measured using time-resolved photoluminescence (PL) decay or transient absorption.[38,39] Transient absorption measurements for P3HT and a variety of fullerenes yield lifetimes between 3 and 6 ns.[38]

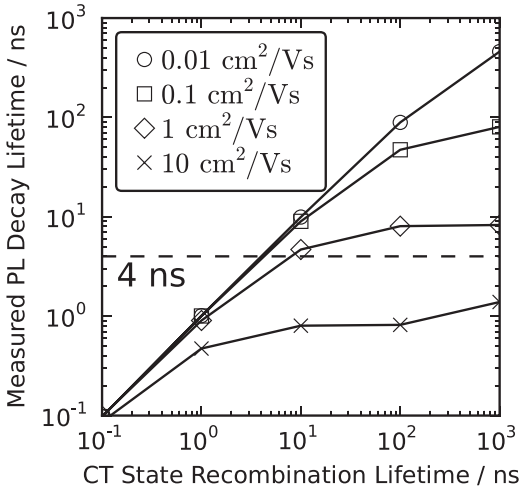

Figure 3. Calibration curve mapping measured geminate pair decay lifetimes to nearest-neighbor recombination lifetimes produced by simulating geminate separation using KMC and extracting the geminate pair lifetime as a function of the value of τ_{ct} input into the simulation for electron and hole mobilities of 0.01, 0.1, 1, and 10 cm^2/Vs ($\mu_e = \mu_h$). The lines are a guide to the eye. The horizontal line represents a typical measured bulk heterojunction CT photoluminescence lifetime of 4 ns.[39]

PL decay measurements of the CT state in PF10TBT:PCBM blends give a lifetime of 4 ns.[39] PL decay measurements are particularly interesting since the technique is directly sensitive to the population of geminate pairs and the decay constant gives the rate at which that population is depleted. However, in high performing BHJ systems, geminate pairs are almost always depopulated by splitting into free charges rather than by recombination. So, the measured polaron pair lifetime is determined by the timescale for recombination and the timescale for dissociation into free carriers, with the timescale for dissociation dominating the measured response. To extract τ_{ct} from these measurements we simulated PL decay curves using KMC for a range of mobilities and recombination lifetimes and calculated from each combination a prediction for the measured lifetime. Our simulations show that the decay remains exponential, as observed experimentally (Supporting Information, Figure S6), but with a modified decay constant. **Figure 3** shows a calibration curve that maps PL lifetimes to CT state recombination lifetimes that can be input into a KMC simulation. For low mobilities, when geminate recombination is likely, the lifetime obtained by a PL experiment and τ_{ct} are similar. However, for high mobilities, such as the local mobilities present in BHJ solar cells, the measured lifetime approaches a limiting value set by the mobility. It is interesting to note that the two measured lifetimes reported in Table 2 (3 and 4 ns) are in good agreement with the limiting values we predict for mobilities between 1 and 10 cm^2/Vs, again reinforcing that local mobilities in BHJ solar cells are on this order and that these are the appropriate values to use when simulating geminate separation. For mobilities between 0.1 and 1 cm^2/Vs, the reported PL decay lifetime of 4 ns would imply an intrinsic CT state lifetime on the order of 1–10 ns. If the carrier mobility were higher, τ_{ct} could also be longer, which would serve to increase the geminate splitting efficiency, so this is a conservative underestimate.

Table 3. Required local mobilities for 90% field-independent IQE for the specified device morphologies.

Morphology	P_{esc}	Required Mobility τ_{ct} = 10 ns
No Mixed Region	1.4×10^{-4}	11 cm^2/Vs
9.6 nm Mixed Region	2.9×10^{-4}	5.1 cm^2/Vs
8 nm Mixed Region	3.5×10^{-4}	4.2 cm^2/Vs
6.4 nm Mixed Region	6×10^{-4}	2.5 cm^2/Vs
4.8 nm Mixed Region	1.3×10^{-3}	1.2 cm^2/Vs
3.2 nm Mixed Region	6.5×10^{-3}	0.23 cm^2/Vs

So far, we have established that geminate splitting in BHJ solar cells, as simulated using KMC is determined by the number of splitting attempts per geminate pair (set by the product $\mu\tau_{ct}$) and the probability that any given attempt is successful (a constant of the energetic landscape we denoted P_{esc}). We can now examine the effect of the mixed region, which alters the energetic landscape, on geminate splitting. The presence of an energy cascade between mixed and aggregated regions means that once a carrier crosses from a mixed to an aggregated region, it is energetically very unlikely to cross back, making the carriers effectively become free after crossing the width of the mixed region, not after traveling 12 nm, as would be predicted with no energy cascade. Reducing the width of the mixed region allows one to systematically increase P_{esc}, thereby greatly improving geminate splitting. Using an estimate for τ_{ct} of 10 ns, and values for P_{esc} obtained from KMC simulations of mixed region widths between 3.2 and 9.6 nm, we can calculate what terahertz mobility would be required for a 90% field-independent IQE in each situation. The results are shown in **Table 3**. For devices with terahertz mobilities above 11 cm^2/Vs we would expect a >90% field independent IQE even without an energy cascade. For lower mobilities down to 0.2 cm^2/Vs (the low end of the range reported in literature for OPV materials), we would still predict a >90%, field-independent IQE, but this high IQE requires a sufficiently thin mixed region with an energy cascade to reduce the distance geminate pairs have to travel before splitting. The results are reported for τ_{ct} = 10 ns, however since we have shown that the splitting efficiency depends on the product $\mu\tau_{ct}$ only, if τ_{ct} were 10 times shorter, the required mobility would simply be 10 times higher.

Since the goal of this manuscript is to explain how geminate pairs split, not to get exact results for a particular material system, we have not taken into account that the splitting probability would depend on where in the mixed region the geminate pair formed. We find that P_{esc} depends primarily on the distance the fastest carrier needs to travel to reach an energy cascade, so if the carriers were formed near a pure fullerene domain, rather than in the center of the mixed region, the hole would have to travel twice as far to reach a pure polymer domain, and P_{esc} could be found by considering a mixed region twice as wide but with the geminate pair formed in the center. On the other hand, if the pair formed near a pure polymer domain, the hole would cross the energy cascade almost immediately. Choosing to have the geminate pair form in the center of the mixed region provides a consistent way to evaluate the impact of mixed region width on geminate splitting.

The question of how BHJ solar cells are able to efficiently generate free charges has persisted for over a decade and many groups have discovered important parts of the explanation like the beneficial role of disorder and the impact of local polarizability and charge carrier delocalization on reducing the geminate pair binding energy. In this communication we build on their work by showing that experimentally measured local charge carrier mobilities and lifetimes in BHJ systems are in the range required for efficient geminate splitting. The picture that emerges of what makes a good BHJ solar cell is a high local charge carrier mobility, long CT state decay lifetime and, when $\mu\tau_{ct}$ is not high enough on its own, a three-phase structure with an energy cascade for either the electron or the hole that increases the probability that a single geminate pair splitting attempt is successful. The combination of these three classes of effects explains how some bulk heterojunctions are able to generate free charges so efficiently. Looking back at Figure 2a, it also explains the wide variability in device performance from system to system since missing any one of these characteristics can be the difference between high, field-independent and low, field-dependent geminate splitting. Importantly, the commonly measured device parameters of bulk mobility and transient absorption lifetimes are shown not to be directly linked to charge generation. Instead we have shown how terahertz mobilities and corrected CT state photoluminescence lifetimes can be used to provide more accurate measurements of the parameters that do determine the efficiency of free charge generation in BHJ solar cells.

Experimental Section

KMC Simulations: All KMC simulations were performed using custom KMC code written by the authors. The First Reaction Approximation was not used. Only single geminate pairs were simulated at a time with open boundary conditions. The world was generated on demand so there was no limit on the size of the simulated lattice. A lattice constant of 8 angstroms was used. The dielectric constant was set at 4 and the temperature was set at 300 K. Each combination of morphology, lifetime, mobility and field was averaged for at least 10000 trials and up to 200000 trials when necessary to capture rare events. For trilayer simulations, the geminate pair was assumed to be formed in the center of the mixed region. The Miller-Abrahams mobility model was used to calculate carrier hopping rates. Each material region was assumed to be homogenous and disorder was not simulated in order to make the simulation amenable to analytical analysis.

PL Decay Simulation: 100000 individual geminate pairs were simulated for each combination of lifetime and mobility and only those that ended in geminate recombination were selected. The time for each recombination event was calculated, binned and histogrammed to produce a simulated PL decay curve. This was fit with a single exponential function to extract the measured lifetime, which was plotted as a function of the actual lifetime input into the simulation. The simulated decays were well fit by single exponential functions (Figure S6). A homogenous morphology was used. The same trilayer morphology described above was tried as well and the results were not greatly sensitive to the change (not shown).

Supporting Information

Supporting Information is available from the Wiley Online Library or from the author.

Acknowledgements

This publication was based on work supported by the Center for Advanced Molecular Photovoltaics (CAMP) (Award No KUS-C1–015–21), made by King Abdullah University of Science and Technology (KAUST). TB was supported by a National Science Foundation Graduate Research Fellowship under Grant No. DGE-1147470. Additional support was provided by Stanford University via a Stanford Graduate Fellowship.

Received: August 22, 2013
Revised: October 11, 2013
Published online: December 27, 2013

[1] Z. He, C. Zhong, S. Su, M. Xu, H. Wu, Y. Cao, *Nat. Photonics* **2012**, *6*, 593.
[2] N. C. Miller, E. Cho, R. Gysel, C. Risko, V. Coropceanu, C. E. Miller, S. Sweetnam, A. Sellinger, M. Heeney, I. McCulloch, J.-L. Brédas, M. F. Toney, M. D. McGehee, *Adv. Energy Mater.* **2012**, *2*, 1208.
[3] B. A. Collins, J. R. Tumbleston, H. Ade, *J. Phys. Chem. Lett.* **2011**, *2*, 3135.
[4] P. Westacott, J. R. Tumbleston, S. Shoaee, S. Fearn, J. H. Bannock, J. B. Gilchrist, S. Heutz, J. DeMello, M. Heeney, H. Ade, J. Durrant, D. S. McPhail, N. Stingelin, *Energy Environ. Sci.* **2013**, *6*, 2756.
[5] B. A. Collins, Z. Li, J. R. Tumbleston, E. Gann, C. R. McNeill, H. Ade, Adv. *Energy Mater.* **2013**, *3*, 65.
[6] S. T. Turner, P. Pingel, R. Steyrleuthner, E. J. W. Crossland, S. Ludwigs, D. Neher, *Adv. Funct. Mater.* **2011**, *21*, 4640.
[7] J. A. Bartelt, Z. M. Beiley, E. T. Hoke, W. R. Mateker, J. D. Douglas, B. A. Collins, J. R. Tumbleston, K. R. Graham, A. Amassian, H. Ade, J. M. J. Fréchet, M. F. Toney, M. D. McGehee, *Adv. Energy Mater.* **2013**, *3*, 364.
[8] C. Groves, *Energy Environ. Sci*. **2013**, *6*, 1546.
[9] Z.-K. Tan, K. Johnson, Y. Vaynzof, A. A. Bakulin, L.-L. Chua, P. K. H. Ho, R. H. Friend, *Adv. Mater.* **2013**, *25*, 4131.
[10] F. C. Jamieson, E. B. Domingo, T. McCarthy-Ward, M. Heeney, N. Stingelin, J. R. Durrant, *Chem. Sci.* **2012**, *3*, 485.
[11] Y. Kim, S. Cook, S. M. Tuladhar, S. a. Choulis, J. Nelson, J. R. Durrant, D. D. C. Bradley, M. Giles, I. McCulloch, C.-S. Ha, M. Ree, *Nat. Mater.* **2006**, *5*, 197.
[12] M. Skompska, A. Szkurłat, *Electrochim. Acta* **2001**, *46*, 4007.
[13] T. J. Savenije, J. E. Kroeze, X. Yang, J. Loos, *Thin Solid Films* **2006**, *511–512*, 2.
[14] T. M. Clarke, J. R. Durrant, *Chem. Rev.* **2010**, *110*, 6736.
[15] B. Kippelen, J.-L. Brédas, *Energy Environ. Sci.* **2009**, *2*, 251.
[16] K. Vandewal, K. Tvingstedt, A. Gadisa, O. Inganäs, J. V Manca, *Nat. Mater.* **2009**, *8*, 904.
[17] S. Rackovsky, H. Scher, *Phys. Rev. Lett.* **1984**, *52*, 453.
[18] H. Scher, S. Rackovsky, *J. Chem. Phys.* **1984**, *81*, 1994.
[19] P. Peumans, S. R. Forrest, *Chem. Phys. Lett.* **2004**, *398*, 27.
[20] T. Offermans, S. C. J. Meskers, R. A. J. Janssen, *Chem. Phys.* **2005**, *308*, 125.
[21] F. C. Jamieson, T. Agostinelli, H. Azimi, J. Nelson, J. R. Durrant, *J. Phys. Chem. Lett.* **2010**, *1*, 3306.
[22] V. Mihailetchi, L. Koster, J. Hummelen, P. Blom, *Phys. Rev. Lett.* **2004**, *93*, 216601.
[23] S. H. Park, A. Roy, S. Beaupré, S. Cho, N. Coates, J. S. Moon, D. Moses, M. Leclerc, K. Lee, A. J. Heeger, *Nat. Photonics* **2009**, *3*, 297.
[24] Y. Liang, Z. Xu, J. Xia, S.-T. Tsai, Y. Wu, G. Li, C. Ray, L. Yu, *Adv. Mater.* **2010**, *22*, E135.
[25] A. A. Bakulin, A. Rao, V. G. Pavelyev, P. H. M. van Loosdrecht, M. S. Pshenichnikov, D. Niedzialek, J. Cornil, D. Beljonne, R. H. Friend, *Science* **2012**, *335*, 1340.
[26] A. E. Jailaubekov, A. P. Willard, J. R. Tritsch, W.-L. Chan, N. Sai, R. Gearba, L. G. Kaake, K. J. Williams, K. Leung, P. J. Rossky, X.-Y. Zhu, *Nat. Mater.* **2013**, *12*, 66.
[27] G. Grancini, M. Maiuri, D. Fazzi, A. Petrozza, H.-J. Egelhaaf, D. Brida, G. Cerullo, G. Lanzani, *Nat. Mater.* **2013**, *12*, 29.
[28] K. Vandewal, S. Albrecht, E. T. Hoke, K. R. Graham, J. Widmer, J. D. Douglas, M. Schubert, W. R. Mateker, J. T. Bloking, G. F. Burkhard, A. Sellinger, J. M. J. Frechet, A. Amassian, M. K. Riede, M. D. McGehee, D. Neher, A. Salleo. *Nat. Mater.* **2013**, 10.1038/nmat3807.
[29] C. Deibel, T. Strobel, V. Dyakonov, *Phys. Rev. Lett.* **2009**, *103*, 1.
[30] B. S. Rolczynski, J. M. Szarko, H. J. Son, Y. Liang, L. Yu, L. X. Chen, *J. Am. Chem. Soc.* **2012**, *134*, 4142.
[31] M. Wojcik, P. Michalak, M. Tachiya, *Appl. Phys. Lett.* **2010**, *96*, 162102.
[32] M. Casalegno, G. Raos, R. Po, *J. Chem. Phys.* **2010**, *132*, 094705.
[33] A. Miller, E. Abrahams, *Phys. Rev.* **1960**, *120*, 745.
[34] R. Noriega, J. Rivnay, K. Vandewal, F. P. V. Koch, N. Stingelin, P. Smith, M. F. Toney, A. Salleo, *Nat. Mater.* **2013**, *12*, 1.
[35] F. Laquai, G. Wegner, H. Bässler, *Philos. Trans. R. Soc., A* **2007**, *365*, 1473.
[36] N. Vukmirovi , C. S. Ponseca, H. N mec, A. Yartsev, V. Sundström, *J. Phys. Chem. C* **2012**, *116*, 19665.
[37] G. Dicker, M. de Haas, L. Siebbeles, J. Warman, *Phys. Rev. B* **2004**, *70*, 045203.
[38] J. H. Choi, K.-I. Son, T. Kim, K. Kim, K. Ohkubo, S. Fukuzumi, *J. Mater. Chem.* **2010**, *20*, 475.
[39] D. Veldman, O. Ipek, S. C. J. Meskers, J. Sweelssen, M. M. Koetse, S. C. Veenstra, J. M. Kroon, S. S. van Bavel, J. Loos, R. A. J. Janssen, *J. Am. Chem. Soc.* **2008**, *130*, 7721.
[40] C. Groves, R. A. Marsh, N. C. Greenham, *J. Chem. Phys.* **2008**, *129*, 114903.
[41] X. Ai, M. C. Beard, K. P. Knutsen, S. E. Shaheen, G. Rumbles, R. J. Ellingson, *J. Phys. Chem. B* **2006**, *110*, 25462.
[42] P. D. Cunningham, L. M. Hayden, *J. Phys. Chem. C* **2008**, *112*, 7928.
[43] H. Nemec, H.-K. Nienhuys, F. Zhang, O. Inganas, A. Yartsev, V. Sundstrom, *J. Phys. Chem. C* **2008**, *112*, 6558.
[44] A. F. Bartelt, C. Strothkämper, W. Schindler, K. Fostiropoulos, R. Eichberger, *Appl. Phys. Lett.* **2011**, *99*, 143304.
[45] C. S. Ponseca, A. Yartsev, E. Wang, M. R. Andersson, D. Vithanage, V. Sundström, *J. Am. Chem. Soc.* **2012**, *134*, 11836.